ELSEVIER

Biophysical Chemistry 132 (2008) 127–138

Biophysical Chemistry

http://www.elsevier.com/locate/biophyschem

Site localization of membrane-bound proteins on whole cell level using atomic force microscopy

Amit Ron [a,*], Ragini Raj Singh [a], Nick Fishelson [a], Rina Socher [b], Dafna Benayahu [b], Yosi Shacham-Diamand [a]

[a] Department of Electrical Engineering Faculty of Engineering, Israel
[b] Department of Cell and Developmental Biology Sackler Faculty of Medicine, Tel-Aviv University, Israel

Received 18 September 2007; received in revised form 31 October 2007; accepted 31 October 2007
Available online 12 November 2007

Abstract

This study presents molecular recognition method, which is based on specific force measurements between modified AFM (atomic force microscopy) tip and mammalian cell. The presented method allows recognition of specific cell surface proteins and receptor sites by nanometer accuracy level. Here we demonstrate specific recognition of membrane-bound Osteopontin (OPN) sites on preosteogenic cell membrane. By merging specific force detection map of the proteins and topography image of the cell, we create a new image (recognition image), which demonstrates the exact locations of the proteins relative to the cell membrane. The recognition results indicate the strong affinity between the modified tip and the target molecules, therefore, it enables the use of an AFM as a remarkable nanoscale tracking tool on the whole cell level.

Keywords: AFM; Force–distance curve; Force spectroscopy; Osteopontin; Preosteogenic cell

1. Introduction

AFM (atomic force microscopy) is a well recognized tool for its high resolution images and also a powerful tool for the detection of Pico scale molecular interactions in variety of applications [1–5]. The ability to detect minute forces provides the possibility to measure and quantify inter molecular forces at the single molecule level [5–8]. From the biological point of view, Pico scale events are used as the primary events in a variety of cell and tissue mechanisms like: tissue development, cell meiosis and replication, stem cell differentiation, signal transduction and many more [9,10]. Interactions at molecular level can be investigated by various force spectroscopy methods [1–3,9,11]. One of the common techniques is based on modified AFM tip, which contains specific ligand such as antibody against the target molecule [4,5,12–15]. Using force–distance measurement it is possible to monitor the changes in interaction level between antibody and target [4,5].

In this study we present an advanced recognition method for biological analysis. The method is based on specific force measurements between modified AFM tip and a mammalian cell. Using this technique we are able to identify the exact location and distribution (by nanometer resolution) of OPN (Osteopontin proteins) over preosteogenic cell membrane. OPN is a secreted glycoprotein which binds to cell surface Integrin receptors and plays a role in mineralization processes [16]. OPN is synthesized by a variety of tissue types including preosteogenic cells, macrophages, and muscle and endothelial cells [17]. OPN plays a role in two major activities: identification of osteoclast cells (bone removing cells) and identification of immune system cells [16,18,19].

The structural mapping can provide information about the distribution of OPN in variety of biological mechanisms like bone formation and destruction, immune system function and behavior, and some cancer types [19]. The presented method is unique in its ability to recognize and locate proteins and receptor sites with resolution of few nanometers, can contribute mostly in the field of cell surface biology and ECM (extra cellular matrix) structure and function. Additionally, this

* Corresponding author. Tel.: +972 3 6406946; fax: +972 3 6423508.
E-mail address: amitron@eng.tau.ac.il (A. Ron).

0301-4622/$ - see front matter © 2007 Elsevier B.V. All rights reserved.
doi:10.1016/j.bpc.2007.10.016

method could be used as analytical tool for different biological applications and as complementary analysis for current methods e.g. immunofluorescence, which have some limitations providing quantitative information about the proteins distribution and their location on the cell.

2. Methods

2.1. Preparation of cells

MBA-15 cells (mouse bone marrow derived preosteogenic cell line) [20] were seeded on round glass cover slips (12 mm in diameter). Cell growth was proceeded in DMEM (Dulbecco's modified Eagle's minimal essential medium) and 10% FCS (fetal calf serum) for 24 h. Fixation was performed using Glutaraldehyde 1.5% in PBS at pH 7.0 for 1 h, three washes; 10 min each were performed in PBS pH 7.0. The cells were stored in phosphate buffer at 4 °C until used. BSA blocking was performed with 5% BSA in PBS prior to AFM analysis.

2.2. Tip functionalization

Cantilevers (Veeco, silicon nitride tips) were cleaned by using sonication in a series of solvents: isopropanol, methanol and deionized water (5 min each). After cleaning, the tips were oxidized by using oxygen plasma (200 W, 1 min, Plasma Preen microwave), after the activation they were transferred into a 2% v/v solution of 3-aminopropyltrimethoxy silane (SIGMA) in toluene for 2 h.

After the silanization process the tips were sonicated in methanol and deionized water (5 min each).

After cleaning, the tips were incubated in a 15% v/v solution of Glutaraldehyde (Grade II, 25% in aqueous solution) in PBS (250 mM, pH 7.0) for 1 h at room temperature. Following incubation the tips were rinsed with PBS to remove the Glutaraldehyde remainders. The tips used for OPN localization were incubated in anti-OPN [19] antibodies solution (0.6 mg/ml in PBS) for 1 h at room temperature. The tips used as control, incubated in IgG antibodies solution (Jackson laboratories, USA), under the same concentration and conditions as the anti-OPN. Following incubation, the probes were rinsed with PBS to remove unattached antibodies. Finally the probes were stored in PBS at 4 °C until used.

2.3. Scan setup

Preosteogenic cell plate was attached to the bottom of the AFM (Pico SPM II, Molecular Imaging) fluid cell and then covered with 200 μl of the cell serum (growth medium). A modified probe which contained anti-OPN antibody was used as recognition sensor during this experiment. The scan parameters which were found as most suitable based on preliminary scans for cell scanning are:

Cantilevers should be relatively soft depending on the cell type and the membrane tension, K values around 0.06 N/m found to be most suitable. The calibration was made using the Thermal tune method [21], where: $K = \frac{K_B T}{\langle Z_C^2 \rangle}$ where K_B is the Boltzmann constant T is the temperature and $\langle Z_C^2 \rangle$ is the mean square displacement of the cantilever.

Force setpoint was taken to be 5 nN; this value could be changed depending on the engage point and membrane tension.

Integral and Proportional gains: Integral gain was 0.2 and Proportional gain was 0.35; these values allowed minimization of noise effects during the scan.

Scan rate was 0.4 lines/s; this scan rate is very useful for big elements and prevents both severe warming of the sample during the scan and better tip tracking especially over heterogeneous surfaces like cell membrane.

Z servo range should be set to maximum (depends on scanner type), 3600 nm during our measurements.

2.4. Calibration of deflection curves

The interpretation of AFM force curves relies almost entirely on established force laws; these force laws describe force as a function of the probe sample separation distance. However, current AFMs, do not have an independent measure of the force $F(d)$, instead, the force is calculated by transforming the deflection signal $V(d)$ using the slope of the cantilever deflection. Therefore, all force curves must be transformed into descriptions of force as a function of distance rather then deflection.

Each deflection curve has been transformed using the following equations:

$$\frac{dZ}{dV} = \frac{Z_{\max} - Z_{\text{contact}}}{V_{\max} - V_{\text{contact}}}$$

and

$$F = kX = k\frac{dZ}{dV}V$$

where $V_{\max}$ is the max deflection signal, V_{contact} is the deflection signal when contact between the tip and the sample is accrued, $Z_{\max}$ is the piezo movement at max deflection and Z_{contact} is the piezo movement at contact point. The determination of Z by this approach requires that the tip makes contact with the sample; in practice there are two factors that can make determining the point of contact very difficult — long range forces and sample elasticity.

Fig. 1 demonstrates two calibrated force–distance curves which have been recorded over preosteogenic cell membrane using anti-OPN coated probe.

2.5. Force–distance measurements

Due to the friction between the tip and the sample, it is impossible to use the modified probes for topography imaging before the recording of force measurements. The modified probes (anti-OPN, anti-IgG) were first used for adhesion measurements of random area on the cell surface, and then immediately used to scan the topography of the same area in identical experimental conditions. Using this methodology, we are able to match the topography and the adhesion detection

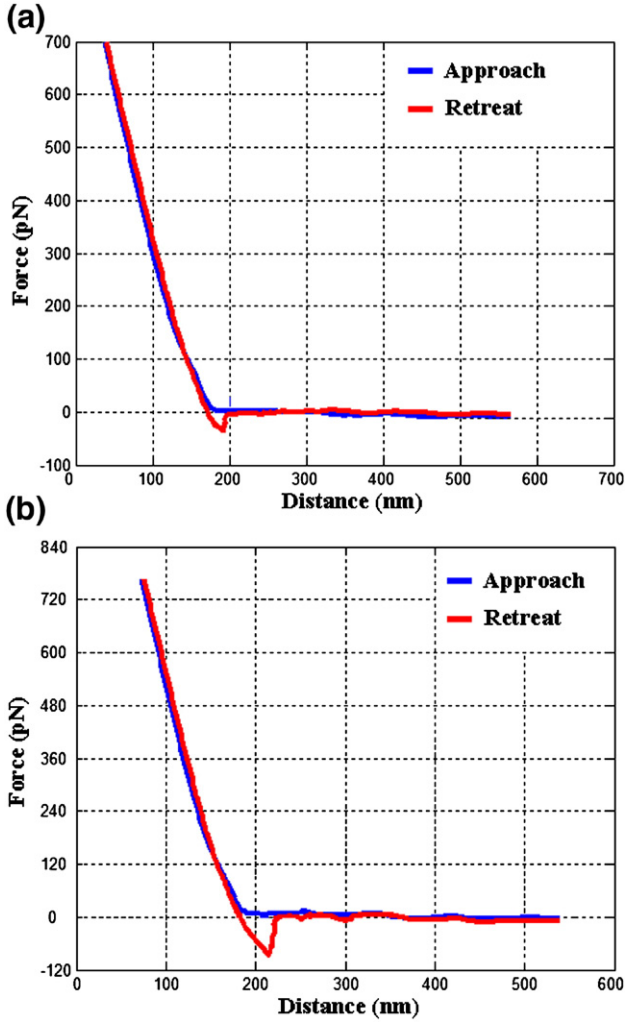

Fig. 1. Force–distance curves demonstrate the adhesion force between the AFM probe and the cell surface (a) low adhesion events (~30 pN) and (b) high adhesion events (~95 pN).

map of the examined area, on the same scale. At the last step, topography of whole cell was recorded in order to set the location of the measured area on cell surface.

Force–volume measurements were recorded using contact force mode over 3 different preosteogenic cells. A rectangular sampling grid was randomly chosen with the spatial segments $\Delta x = \Delta y = 25$ nm (40 × 40 sampling points) scan size 1 μm × 1 μm. Evolution of volume measurements is summarized in Table 1. The mapping characteristics for each measurement are given in Table 2.

Sweep duration for single measurement was set to 3 s which was found most suitable to ensure creation of antibody protein binding during the measurement. The loading rate was 700 pN/s, and was kept constant during both approach and retraction phase. Unlike other ligand receptor complexes, which exhibit higher adhesion as the loading rate increase, here the adhesion force is kept constant at loading rate greater then 700 pN/s. This finding suggests that thermodynamic equilibrium was achieved during the force measurements [22]. Under these setup conditions a constant adhesion frequency of 87% was achieved. The number of data points which has been collected during single measurements was 2000.

2.6. Data analysis

The presented technique is based on numerical matrices to describe and present the force measurement results. The use of matrices, instead of simple two-dimensional curves, makes the recognition process easier. Instead to analyze numerous number of FD curves, equivalent images which are based on the same curves are adapted. Each step during the recognition process is described as a two-dimensional matrix, which is based on a simple 8-bit transformation according to the presented scheme (Recognition method section). The whole analysis process has been performed using MATLAB™ R2006a (The Mathworks Inc.) software.

3. Results

3.1. Detection of recognition events

In this study we describe a multi-image technique which is based on merging of high resolution topographic image and the

Table 1
Summary of force–volume measurements for given probe and cell modifications

Order of measurements	Probe characteristics	Probe modification		Cell treatment	Topography
		Chemical	Biological		
1.	k=0.072 N/m (Calibrated value)	None	None	Fixation	Recorded immediately after force measurements
2.	k=0.074 N/m (Calibrated value)	Silane	None	Fixation	Recorded immediately after force measurements
3.	k=0.074 N/m (Calibrated value)	Silane+Glutaraldehyde	None	Fixation	Recorded immediately after force measurements
4.	k=0.074 N/m (Calibrated value)	Silane+Glutaraldehyde	None	Fixation+BSA blocking	Recorded immediately after force measurements
5.	k=0.074 N/m (Calibrated value)	Silane+Glutaraldehyde	Anti-OPN	Fixation	Recorded immediately after force measurements
6.	k=0.074 N/m (Calibrated value)	Silane+Glutaraldehyde	Anti-OPN	Fixation+BSA locking	Recorded immediately after force measurements
7.	k=0.075 N/m (Calibrated value)	Silane+Glutaraldehyde	Anti-IgG	Fixation	Recorded immediately after force measurements

Table 2
Mapping characteristics of preosteogenic cells

Measurement	Number of tested cells	Mapped segments on each cell	Number of recorded cycles	Duration between sequential cycles
1	3	2	1	–
2	3	2	1	–
3	3	2	1	–
4	3	2	1	–
5	3	3	2	10 min
6	3	3	2	10 min
7	3	3	2	10 min

force detection map of the scanned object. Anti-OPN antibody is attached to the AFM tip prior to the scan. In the case when recognition event between the antibody and the OPN occurs; the AFM detects the "pull-off" (retraction) force which is required to break the interaction between them.

During the recognition process (Fig. 2a) each force–distance curve is transformed to a row of numerical data; the data point which indicates the "pull-off" force between the tip and the sample is isolated and used to the creation of the Force matrix. Every component in the Force matrix represents the "pull-off" value of single retrace curve (the point which refers to the adhesion force between the tip and the sample). Here the number of columns is fitted to the number of sampling points over the *X*-axis and the number of rows is fitted to the number of sampling points over the *Y*-axis. The Force image represents the 8-bit transformation of the Force matrix. It means that every component in the Force matrix has a numerical value within 0 to 255. Here "0" is defined as black coded, meaning the maximum measured force, and "255" as white, meaning the minimum measured force. All the colors within this range are distributed according to the relative force they represent. The color bar is represented by "hot" colors, when the scale is passing

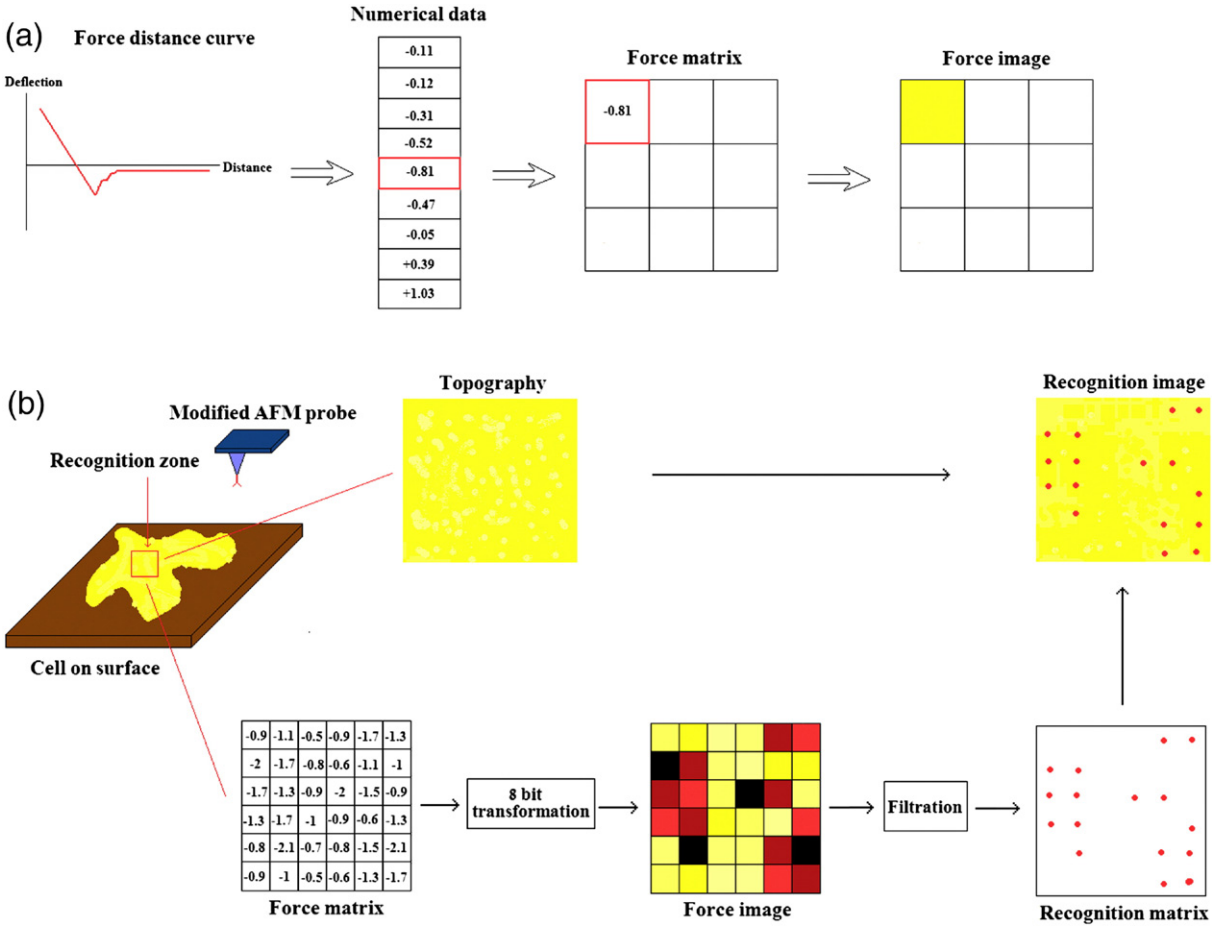

Fig. 2. (a) Scheme of data flow. Each force–distance curve is transformed to a row of numerical data; the value which indicates the unbinding force between the tip and the sample is isolated and inserted to the Force matrix. Every component in the Force matrix represents the adhesion value of single retrace curve. The Force matrix is then transformed using an 8-bit transformation. Every component in the Force image has a numerical value within 0 to 255, which corresponds to a high level of interaction event (dark color) and a low value (bright color) respectively. (b) View of the whole recognition process, from the whole cell to the recognition image. The data which is collected during the scan is used to the creation of both the topography of the scanned cell and the Force matrix. The Force matrix is transformed to an 8-bit representation as was described in Fig. 1a. Numerical filtering process, which is based on the statistical analysis of the force measurements is applied in order to isolate the specific recognition sites from the force image. After the isolation process a new binary matrix is created; each point in the binary matrix (recognition matrix) indicates about the exact location of single target site. The recognition image is created by merging the recognition matrix and the topography image. The location of all target sites (relative to the cell membrane) is demonstrated by the red dots over the image. (For interpretation of the references to color in this figure legend, the reader is referred to the web version of this article.)

through white–yellow–red–black. Therefore, high forces are represented by black and red pixels when the low ones are represented by the white–yellow pixels.

The data collected during the measurement, is inserted into a matrix (Force matrix), which indicates the measured "pull-off" forces over the cell membrane (Fig. 2b). The Force matrix is transformed to an 8-bit representation as described in Fig. 2a. Numerical filtering process, which is based on statistical analysis of the force measurements, is applied in order to isolate the specific recognition sites from the force image. After the isolation process a new binary matrix is created, each point in the binary matrix (recognition matrix) indicates the exact location of single target site. The recognition image is created by merging the recognition matrix and the topography image. The location of all target sites (relative to the cell membrane) is demonstrated by the red dots over the image.

In order to ensure that binding events are related to specific interaction between the anti-OPN modified tip and the free OPN molecules on the cell surface, a series of control measurements were performed. BSA blocking was performed to ensure that unspecific binding events cannot rise from interaction between the modified tip and the cell surface. BSA binds weakly and nonspecifically to number of sites on cell surface, but still allows monitoring specific interactions. Unspecific IgG modified tip, was used to measure the background level of unspecific interaction. In addition, the tip itself was checked during every step of the chemical modification process. This was done in order to monitor the level of interaction between charged areas of the tip and charges on cell membrane.

The final outcome is composed from two images, the topography image of the preosteogenic cell, and an image which displays a map of specific binding interactions between the antibody on the tip, and the target molecules on the cell surface. Through merging the topography image of the cell and the interaction map we create a new image (recognition image), which demonstrates the location of the target molecules (by their coordinates) over the scanned sample.

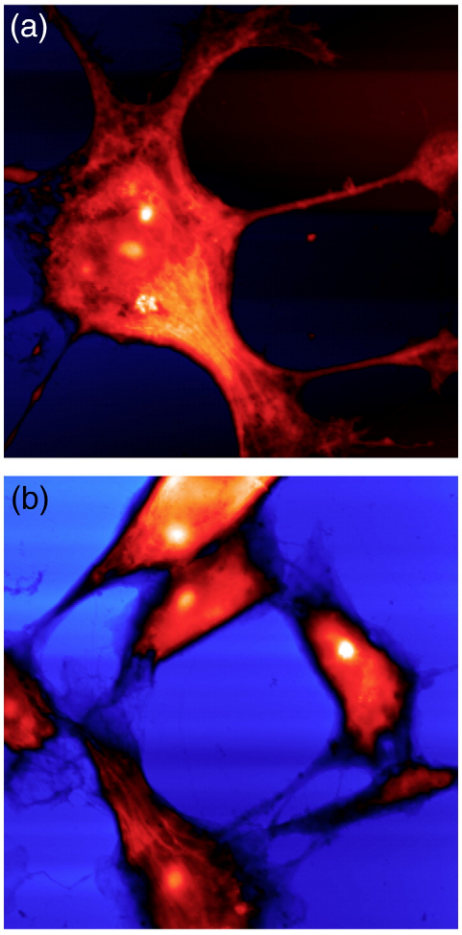

Fig. 3. Two-dimensional topographic images of preosteogenic cells: (a) topography of a single preosteogenic cell (65 μm × 65 μm); (b) topography of joined preosteogenic cells (90 μm × 90 μm).

3.2. Topography scans of Osteoblast cells

High resolution AFM images of living cells are affected by the force which the tip exerted on the sample and the opposite force (from the sample to the tip) which is due to the cell membrane elasticity [23–25]. The topographic images (Fig. 3) demonstrate high resolution structures of analyzed cells. The exact structure of the membrane and small elements such as the cytoskeleton are revealed clearly in those scans. The bright and dark zones in the image indicate the object height relative to the surface; bright zones indicate the high areas and dark zones the low ones. The white areas, which appear on most of the cells, indicate the highest point of the cell which refers to the nucleus and nucleolus locations.

Cross-section analysis revealed information about the average dimensions of these cells:

Average length: 10 μm-60 μm.
Average height above surface: 800 nm–1.2 μm.
Average height of nucleus: 400–600 nm above cell surface.
Average membrane roughness: 300 ± 50 nm.

3.3. Measurement duration

The most crucial factor for recognition based molecular binding is related to the duration of single force measurement (sweep duration). Setting of this value correctly ensures that binding between the modified tip and the target molecules will occur. On the other hand wrong values (too low) will prevent the binding ability. Interactions between antigen and antibody involve noncovalent binding of an antigenic determinant (epitope) to the variable region CDR (complementarity determining region) of both the heavy and light immunoglobulin chains. The binding is mediated by the sum of many weak interactions; these weak interactions include electrostatic attraction/repulsion, Van der Waals attraction, hydrogen bonds, and ionic and/or hydrophobic interactions. These interactions yield different time constant and kinetics, therefore, the whole mechanism of interaction is time dependent, meaning that short sweep duration will reduce the formation of full binding between those two elements. Therefore, it is very

important to ensure that the contact duration between those elements will be high enough to ensure full binding.

In order to set the correct values of binding duration between the OPN and the modified tips (which contain the anti-OPN antibodies), we tested two different sites of OPN on two different preosteogenic cells, prior to the recognition process. In addition, the adhesion frequency (percentage of FD curves with detectable adhesion) was checked over areas which didn't contain OPN molecules.

The specific OPN curves (Fig. 4a and b) demonstrate the development of "pull-off" force as a function of interaction time. It is interesting to notice that both curves possess logarithmic behavior, which is very common for biological systems. Full binding between OPN and its antibody occurs when the interaction time is become larger then 0.75 s, which is equal to sweep duration of 3 s. After this period, the curve reaches the plateau phase, which means that the "pull-off" force between those two elements stays approximately constant. The relatively long interaction time is very common for bio-membrane force probe techniques, which usually require long period of loading ($1–10^3$ pN/s) in order to achieve high sensitivity [26].

The adhesion frequency plot (Fig. 4), reveals that most adhesion events (87%) are detectable at sweep duration greater then 1.2 s. This finding suggests that unspecific adhesion events can be measured at short duration comparing to the specific ones. Meaning that adhesion frequency alone cannot provide reliable data regarding the optimal sweep duration of the FD measurement. To obtain the true duration, the specific adhesion between the modified probe and the desirable site on the surface must be checked separately; otherwise, the probability of unspecific adhesion events will increase significantly, therefore, specific adhesion events will be out of detection range.

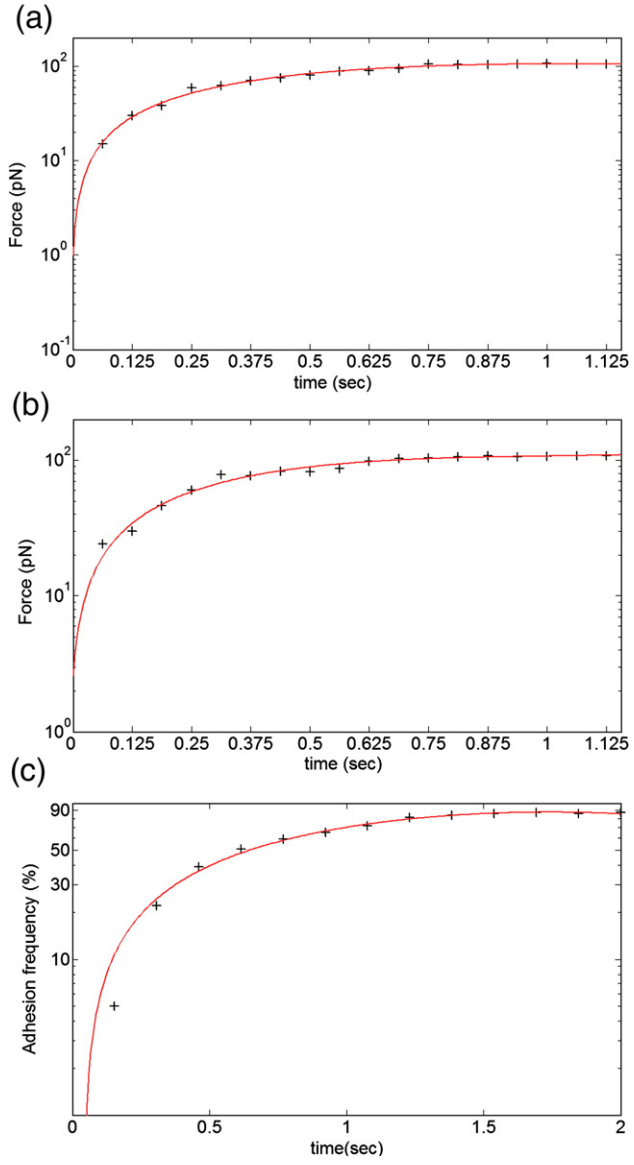

Fig. 4. Plots (a) and (b) demonstrate the change in "pull-off" force between OPN and antibody as function of interaction time. Plot (c) demonstrates the adhesion frequency as function of sweep duration.

3.4. Analysis of adhesion events

The measured adhesion forces can rise from several interaction mechanisms between the tip and the cell surface. The major interactions, which contribute/appear mostly during single molecule experiments, are summarized in Fig. 5. The level of adhesion interaction was measured through a series of probe modifications in order to evaluate the effect of background interferences on the specific interaction of OPN. In addition, the level of unspecific binding was checked through the use of unspecific IgG antibody, and BSA blocking treatment of the cell surface. Table 3 summarizes the evolution of adhesion measurements during all the modification steps.

The bare tip measurements (Fig. 6a and h) reveal that the average adhesion force between the silicon probe and the cell membrane is 21±7 pN (mean±STD). In the case of Silane (Fig. 6b and i) and Silane+Glutaraldehyde (Fig. 6c and j) modification, the average adhesion values have been found in the range of 29±14 pN and 27±12 pN respectively. The relative shift in both distribution and adhesion levels is probably attributed to charge interaction between charged groups on the tip and the cell surface. Untreated areas on the tip (which have substantial negative charge SiO^-), amino silane (which has substantial positive charge NH_3^+), unreacted Glutaraldehyde or hydrolyzed Glutaraldehyde (COO^-), can react with charges on the surface, for example, charged amino acid residues on membrane proteins. When BSA was added to the cell culture (Fig. 6d and k), the average adhesion value was found in the range of 23±8 pN, which is similar to the value measured with the bare tip. Here most of the charge interactions have been blocked as a direct result of the cell surface blocking.

The use of anti-OPN probe (Fig. 6e and l), demonstrates clear separation between two populations of "pull-off" events (5–56 pN, 67–145 pN). The left population (5–56 pN) is related to interactions between the modified OPN probe and "clean" spots on the cell surface, which is quite similar to the one measured with the bare tip. The right population (67–145 pN), contains information on both specific and unspecific interactions. Part of those interactions can be tagged as specific binding between the anti-OPN coated probe and OPN sites on

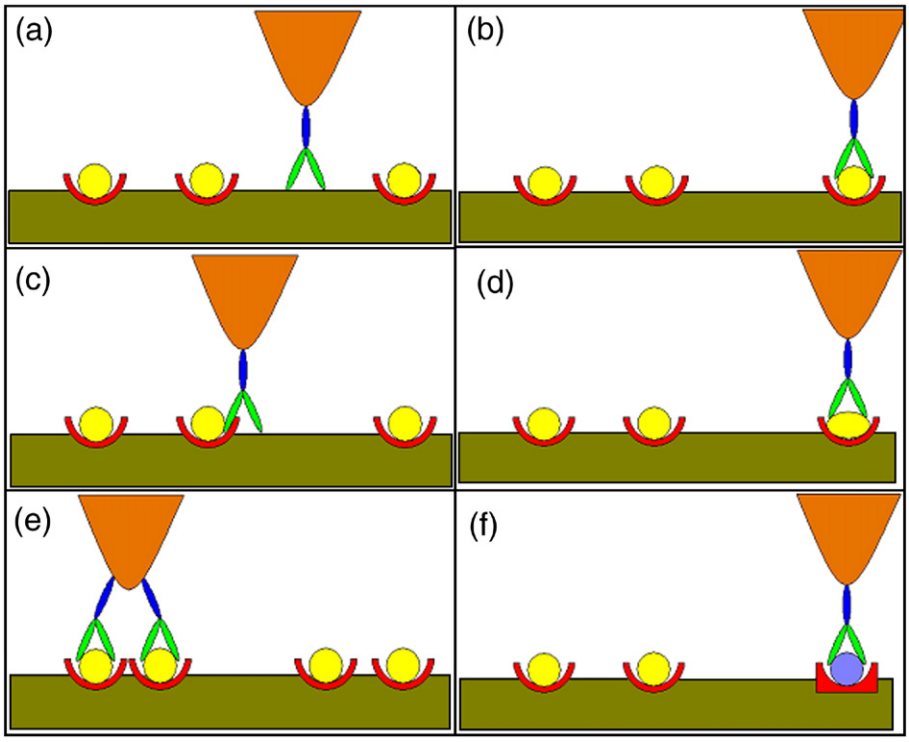

Fig. 5. Tip sample interactions: (a) tip surface interaction, which mostly motivated by Van der Walls and electrostatic interactions; (b) antibody–antigen binding interaction, demonstrates binding between the antibody coated probe and the target molecule on the surface; (c) partial binding interaction, usually takes place when the tip is approaching toward a point which is located near the antigen site but not on the exact location; (d) interaction by unsuitable conformation, when the antigen reveals a wrong primary or secondary structure, the affinity to its matching antibody can be reduced dramatically; (e) multiple binding interaction, occurs when several antibodies glued to the AFM tip during the functionalization process. When the tip is approaching toward a point which is close to several target sites, the possibility of simultaneous binding can be increased, meaning that several recognition events will take place simultaneously; (f) unspecific binding, this event can occur when two or more molecules exhibit very similar structural conformation comparing to the target molecules. Here the binding possibility between the coated probe and those molecules is increased; therefore, unspecific binding events can occur.

the cell surface, while the others can rise from several mechanisms as described before in Fig. 4.

Evaluation of unspecific interactions was performed using BSA blocking and unspecific IgG antibody, as performed traditionally in many biological binding assays [27]. When the cell surface was blocked by BSA (Fig. 6f and m), the adhesion range was reduced to value of 73–125 pN. Meaning that significant change in the high level interactions has been appeared. Respectively, the average adhesion value was found to be 94±11 pN comparing to 107±16 pN before the blocking. This change can be related to blocking of unspecific and charged sites on the cell membrane, which brought to reduction in high adhesion events.

The use of unspecific IgG was designed in order to quantify the level of binding between unspecific modified probe and receptor sites on the cell membrane. The use of unspecific antibody is very important in many biological assays; it can provide true indication regarding random and unspecific binding. Here we used IgG (Fig. 6g and n) to evaluate the level of unspecific binding between the anti-OPN and unspecific sites on the membrane. Here the adhesion was found in the range of 9–73 pN, with an average adhesion of 32±12 pN, which indicates that most unspecific binding events yield low adhesion values. This can suggest low contribution of unspecific binding between the anti-OPN and unspecific sites on the membrane. It means that binding between the anti-OPN

Table 3
Statistical analysis of adhesion measurements for given probe and cell modifications

Probe modification	Surface blocking	Adhesion range (pN)	Mean adhesion value (x)	Standard derivation (σ)	Reference
Without (bare tip)	None	5–51	21	7	Fig. 6(a and h)
Silane	None	7–62	29	14	Fig. 6(b and i)
Silane+Glutaraldehyde	None	9–58	27	12	Fig. 6(c and j)
Silane+Glutaraldehyde	BSA	7–53	23	8	Fig. 6(d and k)
Anti-OPN	None	5–56, 67–145	26, 107	11, 16	Fig. 6(e and l)
Anti-OPN	BSA	7–55, 73–125	24, 94	9, 11	Fig. 6(f and m)
Unspecific IgG	None	9–73	32	12	Fig. 6(g and n)

and unspecific sites on the membrane, probably, does not effect significantly on the recognition ability of OPN.

3.5. Localization of OPN sites

The adhesion values of several force curves contain information about OPN recognition at the level of single molecule interaction (specific recognition events). Isolation of those specific events enables localization of the exact OPN sites on the cell membrane. The localization process is based on isolation of specific segment ("recognition frame") from the OPN histogram, which mostly contains data regarding specific interaction of OPN. The boundaries of the frame are important factors, which influence both recognition yield and error, and therefore, should be set carefully.

Analysis of the force histograms reveals that most of the high adhesion events are located at the range of 90–120 pN. Those events represent 70% of the total events which demonstrate adhesion value greater than 70 pN. Therefore, based on the high affinity between OPN and its matching antibody, we can assume that most of the specific binding events are located within this range. Also, in both control experiments (BSA blocking, IgG), this range was found to be "clean" from the presence of unspecific events.

In order to develop a criterion regarding the setting of the correct recognition frame, we performed a series of force experiments between randomly distributed Lysozyme proteins and anti-Lysozyme coated probe. Based on those results, we found that suitable recognition frame for protein molecules is found mostly at the range of ±10 pN around the average adhesion force (here the mean was calculated based on adhesion events greater then 75 pN). Using this frame, we achieved recognition of ~85% of the molecules, and recognition error of ~8% (only one of 12 recognition events was considered false). Also, previous single molecule studies investigated the average binding force between different pairs of antibody and antigen, which is found within the range of ±10–20 pN around the mean binding force [4,5].

Based on the OPN measurements, we found that the average adhesion force between the anti-OPN coated probe and the cell surface is 107±16 pN. When the measurement performed with the presence of BSA, (which minimized the effect of unspecific

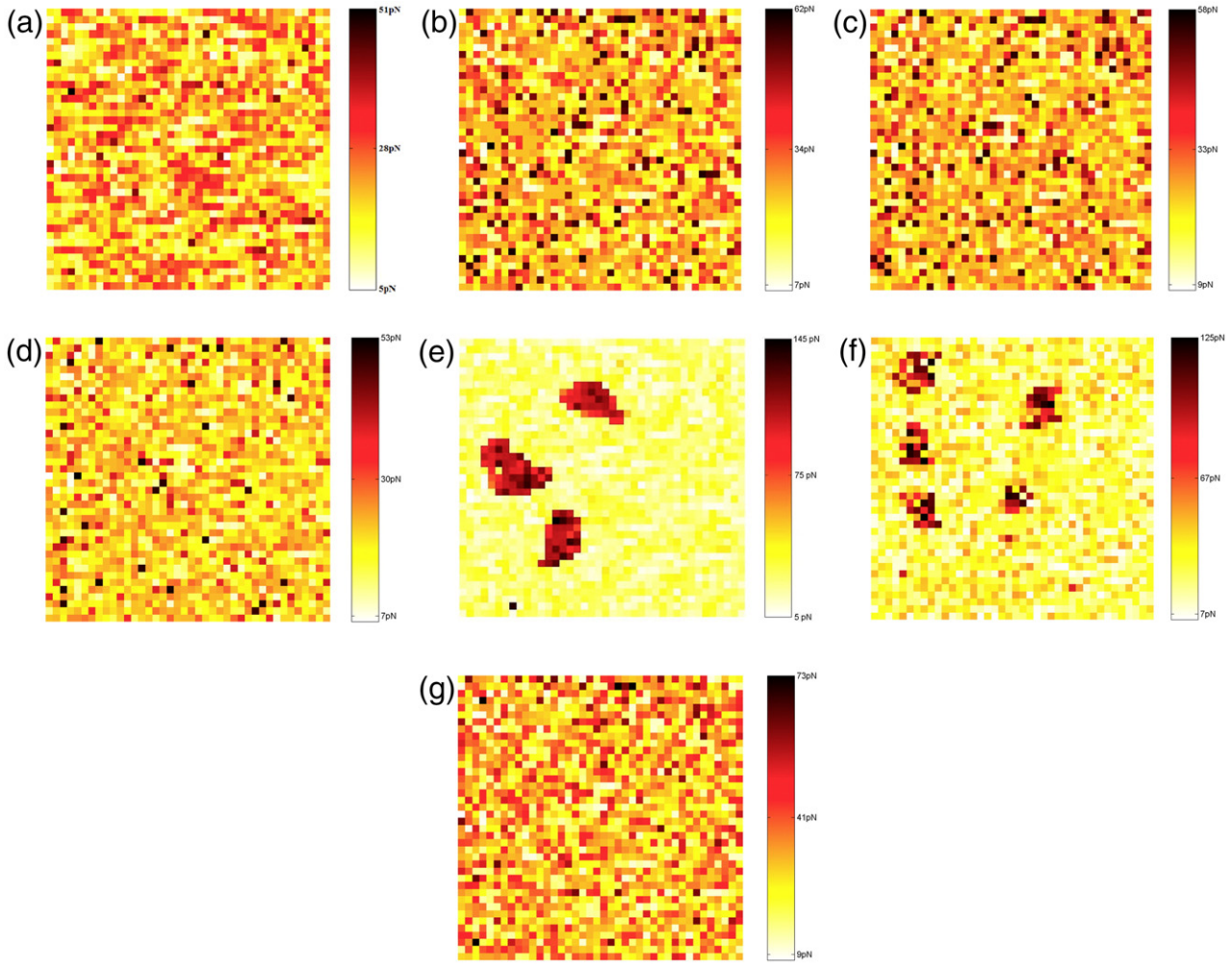

Fig. 6. Force images (a–g) demonstrate the distribution of "pull-off" forces over preosteogenic cell membrane after a series of experiments as shown in Table 2. The level of brightness indicates the level of "pull-off" interaction over the matching area on cell membrane. The related histograms (h–n) demonstrate the adhesion distribution for the corresponding force images.

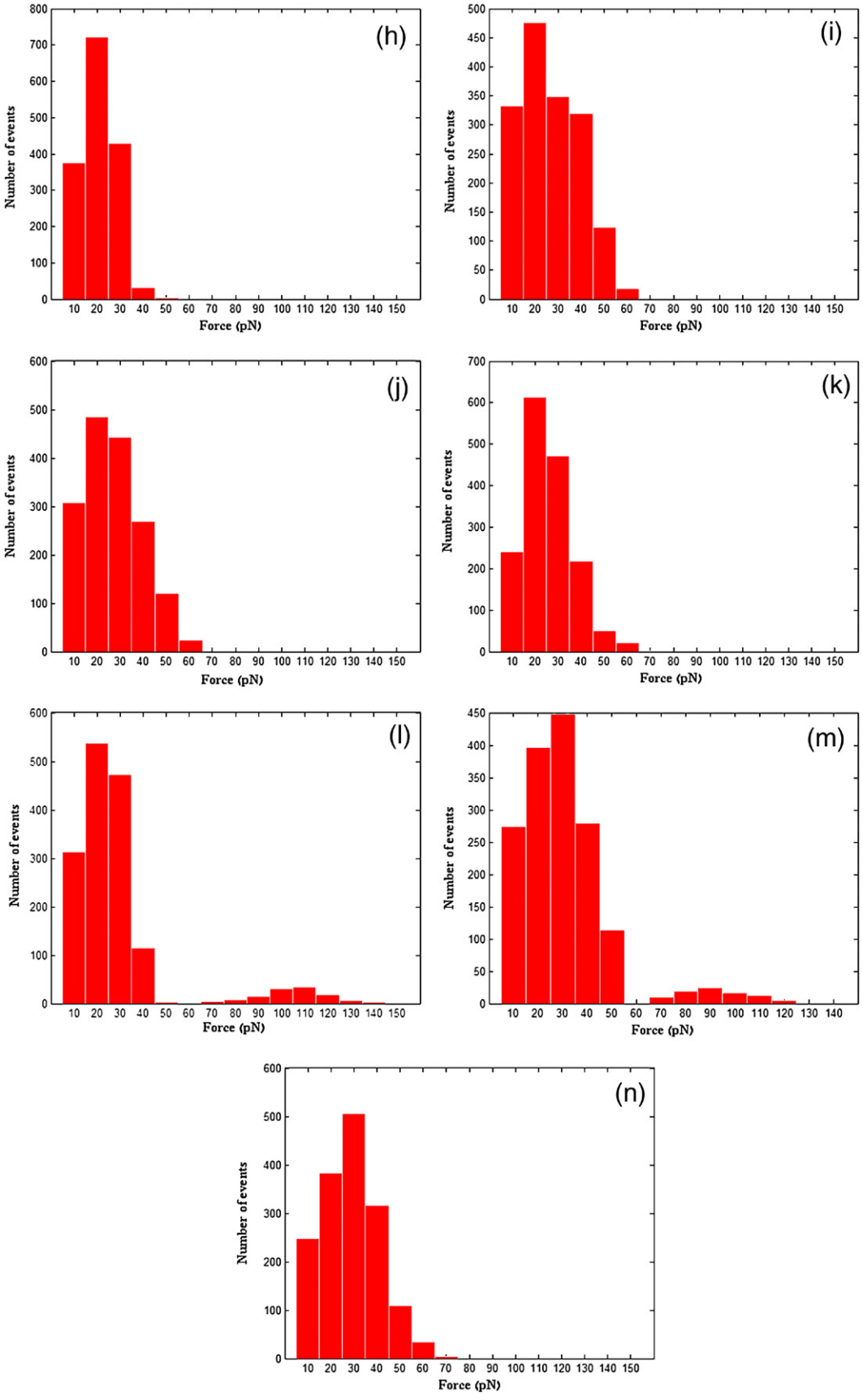

Fig. 6 (*continued*).

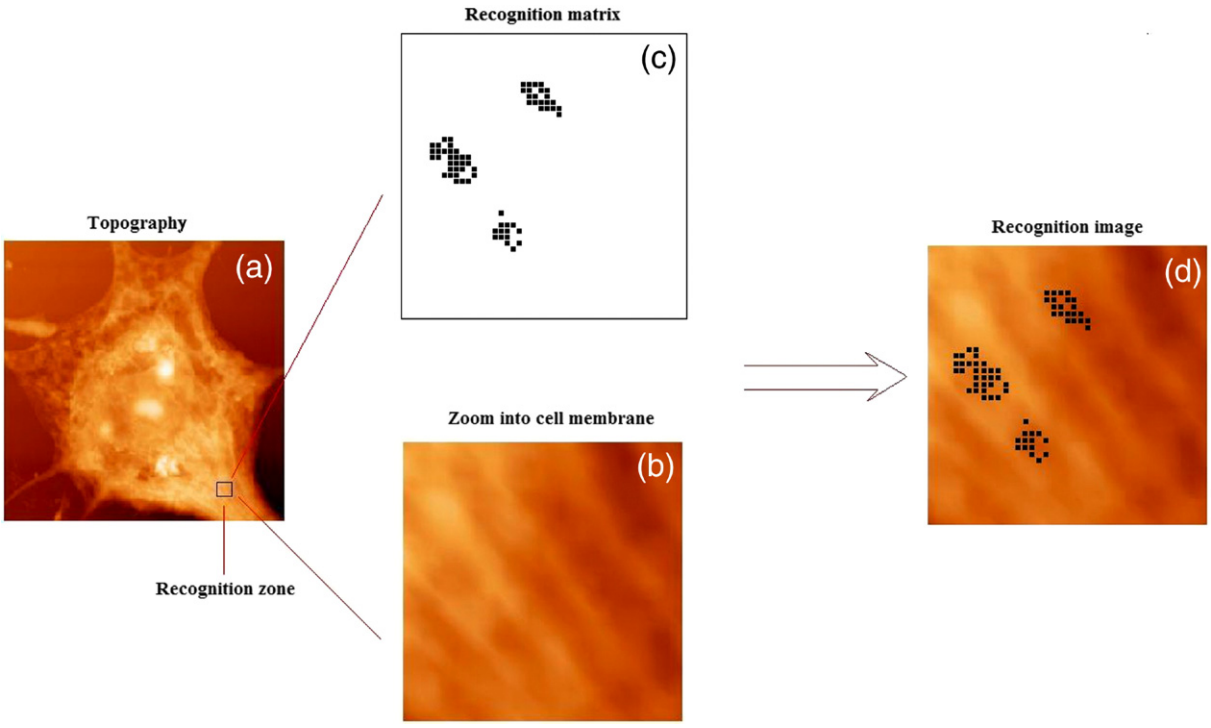

Fig. 7. (a) AFM image demonstrates the topography of the whole preosteogenic cell (30 μm×30 μm). The black frame on the right corner (1 μm×1 μm) shows the chosen recognition zone. (b) High resolution topography of recognition zone. (c) Recognition matrix demonstrates the location of all specific binding events between anti-OPN tip and the OPN proteins on the cell surface. (d) The recognition image was created by merging the binary matrix and high resolution topography of the recognition zone. (image b+image c) The image reveals the location of all OPN sites over the recognition zone; each black point indicates the location of single OPN site.

events) the average adhesion was 94±11 pN. Hence, the probability to find the mean binding force of OPN within the range of 94–107 pN, considered high. In order to achieve high recognition yield we preferred to choose a relatively wide recognition frame. Such a frame provides high tolerance on one hand and high recognition yield on the other. In other words, we preferred to achieve recognition of most receptor sites even if some of the sites are not the true sites (unspecific events). Therefore the recognition frame was chosen to be 100±15 pN. Using this frame we still keep on the mean binding force of OPN, and also minimize the affects of unspecific events on the recognition accuracy.

After the setting, each pixel in the force image is compared to the limitation values of the frame. If the value is located within the frame the pixel is considered as a specific interaction and will get the binary value "1", otherwise, the value will be "0". The binary image (Fig. 7c) which is known as "recognition matrix" demonstrates the exact location of all OPN sites relative to the measurements order. The recognition image (Fig. 7d) has been created by merging the recognition matrix (Fig. 7c) and high resolution topography of cell membrane (Fig. 7b) which is a part from the whole preosteogenic cell (Fig. 7a). The image demonstrates the exact location of OPN sites relative to the cell membrane.

4. Discussion

AFM is a powerful tool for exploring the forces and the dynamics of the interaction between individual ligands and receptors, either on isolated molecules or on cellular surfaces [8,9]. Studies on the single molecule level are implemented using AFM force spectroscopy techniques [1,2,4]. Spectroscopy technique allows quantifying the molecular interaction between the AFM tip and the target molecules on the surface [2,11]. The results presented in this study, highlight the wide potential of AFM force spectroscopy also as a tool for nanometer functional mapping on the single cell level.

Previous AFM studies demonstrated spectroscopy analysis of membrane proteins on microbial and yeast cells [28–30]. The study of mammalian cells is therefore challenging for such analysis and thus the results presented here are new. The resolution at the nanometer scale provides information about function-related protein existence on the surface of live cells. The mapping of membrane proteins relies on quantification of force distribution and probing after specific recognition forces at the surface of living cells. This unique mapping provides a new insight into the molecular mechanisms of cell membrane structure. In addition, such analysis provides an enhanced knowledge of cell adhesion, interaction with other cells and ECM that regulates cell growth and differentiation. Knowledge about the surface properties of cells is a key to understand their functions in cell–cell interaction and the environmental effects that exploit them in differentiation process.

During this study we tracked after the distribution of OPN over preosteogenic cell membrane. By mapping the adhesion forces between anti-OPN coated probe and the cell surface; we were able to recognize specific OPN nanodomains over the cell membrane. The measured adhesion force and time (sweep and

frequency) suggests that the formation of anti-OPN–OPN binding is probably based on creation of several intermolecular bridges/mechanisms. OPN is an open, flexible molecule, in part because of the abundance of negative charges resulting from many acidic amino acids, and multiple Phosphoserines, distributed along its length [31]. The relative long binding time (~3 s), is therefore due to some conformational changes occur in order to allow the full binding between the negative domains on the OPN and the positive ones on its antibody.

The distribution of adhesion forces reveal clear separation between high and low events, which can be attributed/translated to OPN localization over the membrane. Low adhesion events (10–50 pN) may correspond to interaction between the coated probe and non/low reactive domains on the membrane. The high events (85–135 pN, ~80% of the high adhesion measurements) rise from both specific and unspecific interactions of anti-OPN with the cell surface. Based on the high affinity of OPN, which is one of the highly conserved proteins among vertebrates and the unspecific IgG control, the probability of unspecific binding (false sites) seems low. On the other hand, the BSA control, which eliminates contributions from non-specific binding interactions, suggests possible contribution of charge interactions which can yield (in addition to anti-OPN specific binding) high adhesion values. The mid rang values (70–80 pN, ~10% of the high adhesion measurements), which were not affected from both the controls, were probably raised from partial/unsuitable binding interaction (Fig. 5c and d) and therefore exhibit relative decrease in adhesion.

OPN contains a conserved RGD (Arg-Gly-Asp) sequence, and bind to preosteogenic cells via Integrin-mediated mechanisms [31–33]. Therefore, the distribution of OPN can be referred to specific sites, which demonstrate binding with Integrin receptors. The recognition image (Fig. 7d) reveals the distribution and location of OPN–Integrin complexes over preosteogenic cell membrane. These complexes exhibit strong tendency to arrange in several groups, which are located mainly between the cytoskeleton filaments. It is interesting to reveal that Integrin receptors (which have been considered as one of the important receptor groups) are expressed, mostly over flat regions of the cell membrane; this unique expression may enhance their ability to bind their substrate. The relatively high number of Integrin receptor is not so surprising due to the high number of cell activities, which are controlled by the Integrin family. Most of these activities are related to signal transduction, which is very important to cell function and surviving [34].

The feasibility of force measurements on preosteogenic cells has been demonstrated in this study using the anti-OPN antibodies and can be expanded to mapping of any cell surface proteins. Also, it can be combined with biochemistry and molecular analysis. The presented technique offers unique advantages for molecular recognition:

1) High sampling resolution which leads to high tracking ability after target molecules on cells,
2) High recognition specificity, which rises from the ability to monitor single event during single force measurement,
3) Tracking after the real behavior of the object due to the natural imaging conditions which mimic real biological environment,
4) No need of sample pretreatment and therefore less sample damage,
5) Clear and simple output which demonstrates the true location of target molecules on the surface of the scanned object.

These and other characteristics make AFM a powerful tracking tool to follow single biological molecule. The ability to demonstrate the real location of single molecule over the cell membrane (or in a tissue), offering a wide range of opportunities for advance research in a single molecule level, and can also provide unique insights into the mechanisms of cell physiology.

Acknowledgment

CellProm project, FP6th of the European Community (NMP4-CT-2004-500039).

References

[1] H. Clausen-Schaumann, M. Seitz, R. Krautbauer, H.E. Gaub, Force spectroscopy with single bio-molecules, Curr. Opin. Chem. Biol. 4 (2000) 524–530.
[2] B. Heymann, H. Grubmuller, Dynamic force spectroscopy of molecular adhesion bonds Phys. Rev. Lett. 84 (2000) 6126–6129.
[3] P. Bongrand, Ligand receptor interactions, Rep. Prog. Phys. 62 (1999) 921–968.
[4] Z. Jordanka, M.L. Stuart, H.L. Sanford, Single molecule force spectroscopy in biology using the atomic force microscope, Prog. Biophys. Mol. Biol. 74 (2000) 37–61.
[5] L. Shiming, C. Ji-Liang, H. Long-Sun, L. Huan-We, Measurements of the forces in protein interactions with atomic force microscopy Curr. Proteomics 2 (2005) 55–81.
[6] W.W. John, S. Henry, I.L. Rustem, Protein–protein unbinding induced by force: single-molecule studies, Curr. Opin. Struct. Biol. 13 (2003) 227–235.
[7] R. Anneliese, W. Han, D. Badt, S.J. Smith-Gill, S.M. Lindsay, H. Schindler, P. Hinterdorfer, Antibody recognition imaging by force microscopy Nat. Biotechnol. 17 (1999) 902–905.
[8] F.H. William, H.H. Jan, Spatially resolved force spectroscopy of biological surfaces using the atomic force microscope Nanotechnology 17 (1999) 143–150.
[9] J.L. Alonso, W.H. Goldmann, Feeling the forces: atom force microscopy in cell biology, Life Sci. 72 (2003) 2553–2560.
[10] D. Leckband, J. Israelachvili, Intermolecular forces in biology, Q. Rev. Biophys. 34 (2001) 105–267.
[11] H.J. Butt, M. Jaschke, W. Ducker, Measuring surface forces in aqueous solution with the atomic Force microscope Bioelectrochem. Bioenerg. 38 (1995) 191–201.
[12] H. Peter, B. Werner, J.G. Hermann, S. Kurt, S. Hansgeorg, Detection and localization of individual antibody–antigen recognition events by atomic force microscopy Proc. Natl. Acad. Sci. U. S. A. 93 (1996) 3477–3481.
[13] A. Stephanie , C. Xinyong, D. John, D.C. Martyn, C.D. Adrian, C.E. John, J.R. Clive, S. Joanna, T.J.B. Saul, W.M. Philip, Detection of antigen-antibody binding events with the atomic force microscope Biochemistry 36 (1997) 7457–7463.
[14] S. Wielert-Badt, P. Hinterdorfer, H.J. Gruber, J.T. Lin, D. Badt, B. Wimmer, H. Schindler, R.K.-H. Kinne, Single molecule recognition of protein binding epitopes in brush border membranes by force microscopy, Biophys. J. 82 (2002) 2767–2774.
[15] W. Baumgartner, P. Hinterdorfer, W. Ness, A. Raab, D. Vestweber, H. Schindler, D. Drenckhahn, Cadherin interaction probed by atomic force microscopy, Proc. Natl. Acad. Sci. U. S. A. 97 (2000) 4005–4010.

[16] H. Yoshitake, S.R. Rittling, D.T. Denhardt, M. Noda, Osteopontin-deficient mice are resistant to ovariectomy-induced bone resorption, Proc. Natl. Acad. Sci. U. S. A. 96 (1999) 8156–8160.
[17] L.F. Brown, B. Berse, L. Van de Water, A. Papadopoulos-Sergiou, C.A. Perruzzi, E.J. Manseau, H.F. Dvorak, D.R. Senger, Expression and distribution of osteopontin in human tissues: widespread association with luminal epithelial surfaces, Mol. Biol. Cell 3 (1992) 1169–1180.
[18] M.F. Young, J.M. Kerr, J.D. Termine, U.M. Wewer, M.G. Wang, O.W. McBride, L.W. Fisher, cDNA cloning, mRNA distribution and heterogeneity, chromosomal location and RFLP analysis of human osteopontin (OPN), Genomics 7 (1990) 491–502.
[19] R. Marom, I. Shur, R. Solomon, D. Benayahu, Characterization of adhesion and differentiation markers of osteogenic marrow stromal cells, J. Cell. Physiol. 202 (2005) 41–48.
[20] D. Benayahu, Y. Kletter, D. Zipori, S. Wientroub, Bone marrow-derived stromal cell line expressing osteoblastic phenotype in vitro and osteogenic capacity in vivo, J. Cell. Physiol. 140 (1989) 1–7.
[21] J.L. Hutter, J. Bechhoefer, Calibration of atomic-force microscope tips, Rev. Sci. Instrum. 64 (1993) 1868–1873.
[22] A. Tommaso, R. de Jong Menno, M. Alart, C.J.M. van Veggel Frank, H. Jurriaan, R.N. David, Z. Shan, Z. Szczepan, S. Holger, G.J. Vancso, K. Laurens, β-Cyclodextrin host–guest complexes probed under thermodynamic equilibrium: thermodynamics and AFM force spectroscopy, J. Am. Chem. Soc. 126 (2004) 1577–1584.
[23] C. Zhu, B. Gang, N. Wang, Cell mechanics: mechanical response, cell adhesion, and molecular deformation Annu. Rev. Biomed. Eng. 12 (2000) 189–226.
[24] P.P. Lehenkari, G.T. Charras, A. Nykanen, M.A. Horton, Adapting atomic force microscopy for cell biology, Ultramicroscopy 82 (2000) 289–295.
[25] K. Schilcher, P. Hinterdorfer, H.J. Gruber, H.A. Schindler, Non invasive method for the tight anchoring of cells for scanning force microscop Cell Biol. Int. 21 (1997) 769–778.
[26] E. Evans, K. Ritchie, Dynamic strength of molecular adhesion bonds, Biophys. J. 72 (1997) 1541–1555.
[27] B. Alberts, D. Bray, A. Johnson, J. Lewis, M. Raff, K. Roberts, P. Walter, Essential Cell Biology: An Introduction to the Molecular Biology of the Cell, Garland publishing inc., 1998.
[28] Y.F. Dufrene, C.J.P. Boonaert, P.A. Gerin, M. Asther, P.G. Rouxhet, Direct probing of the surface ultrastructure and molecular interactions of dormant and germinating spores of phanerochaete chrysosporium J. Bacteriol. 181 (1999) 5350–5354.
[29] A. Touhami, B. Hoffmann, A. Vasella, F.A. Denis, Y.F. Dufrene, Aggregation of yeast cells: direct measurement of discrete lectin–carbohydrate interactions, Microbiology 149 (2003) 2873–2878.
[30] V. Dupres, F.D. Menozzi, C. Locht, B.H. Clare, N.L. Abbott, S. Cuenot, C. Bompard, D. Raze, Y.F. Dufrene, Nanoscale mapping and functional analysis of individual adhesions on living bacteria, Nat. Methods 2 (2005) 515–520.
[31] O. Ake, F. Ahnders, H. Dick, Cloning and sequence analysis of rat bone sialoprotein (osteopontin) cDNA reveals an Arg-Gly-Asp cell-binding sequence, Proc. Natl. Acad. Sci. U. S. A. 83 (1896) 8819–8823.
[32] D.T. Denhardt, X. Guo, Osteopontin: a protein with diverse functions, FASEB J. 7 (1993) 1475–1482.
[33] D.D. Hu, J.R. Hoyer, J.W. Smith, Ca^{2+} suppresses cell adhesion to osteopontin by attenuating binding affinity for integrin alpha v beta 3, J. Biol. Chem. 270 (1995) 9917–9925.
[34] A. Teti, Regulation of cellular functions by extracellular matrix, J. Am. Soc. Nephrol. 2 (1992) 83–87.